J13.3 DEPENDENCE OF PEAK DAILY OZONE CONCENTRATIONS IN HOUSTON, TEXAS ON THE SEA BREEZE AND METEOROLOGICAL VARIABLES

Robert M. Banta[1], C.J. Senff[1,2], R.J. Alvarez[1], D.D. Parrish, M.K. Trainer, T.B. Ryerson, L.S. Darby, R.M. Hardesty, B. Lambeth, J.A. Neuman, W.M. Angevine, J.W. Nielsen-Gammon[3], S.P. Sandberg, A.O. Langford, and A.B. White[1]

[1] Earth System Research Laboratory (ESRL), NOAA, Boulder, CO, U.S.A.
[2] Cooperative Institute for Research in Environmental Sciences (CIRES), Boulder, CO, U.S.A.
[3]Texas Commission on Environmental Quality, Austin Texas
[4]Texas A&M University, College Station, Texas

Introduction. Understanding atmospheric conditions that lead to high concentrations of air pollutants is important for being able to predict high-pollution days, to interpret air-chemistry measurements, and to assess the performance of numerical weather prediction (NWP) models. Concentrations of secondary photochemical pollutants such as ozone depend on emission source strength, chemical reactions, and the role of meteorological processes, particularly in diluting the emissions or allowing them to accumulate. In general, day-to-day variability in peak pollutant concentrations reflect meteorological variability, since emission source activity tends to be more similar from one day to the next (except for industrial spills or "upsets," which happen occasionally but unpredictably). This study is aimed at characterizing warm-season meteorological conditions that contribute most strongly to this daily variability, especially those conditions associated with high ozone concentrations, in the urban-industrial region near Houston, Texas.

The Houston area is the hub of one of the major air pollution source regions in the United States, as a result of a unique mix of pollution-emission activities combined with summertime meteorology dominated by irregular coastline effects. Pollution sources include petrochemical plants, which lie along the Ship Channel, along the western shore of Galveston Bay (Fig.1), and in other locations; the Houston urban area; power plants; and shipping activity in Galveston Bay and the Ship Channel (Williams et al. 2009). Summertime meteorological conditions in this coastal location feature routine occurrences of the daytime sea breeze along the Gulf of Mexico shoreline and inland (Fig. 1b). On days when larger-scale winds in the lower boundary layer (BL) are offshore and not too strong, the diurnal sea-breeze cycle produces midday reversals of the wind direction. "Not too strong" here would generally mean less than about 3 m s^{-1}. During such reversals, 1-2 hr periods of stagnation often occur along the sea-breeze front, resulting in accumulations of high pollution concentrations (SAI et al., 1995, Banta et al 2005, Darby 2005).

To better understand the chemical and meteorological processes producing the high pollutant concentrations, two measurement campaigns, the Texas Air Quality Studies, were carried out during the summer pollution seasons of 2000 and 2006 (TexAQS-2000 and TexAQS-2006). Between the campaigns—and in part as a result of findings from the 2000 study—a number of emission-control measures were implemented. For example, evidence has been presented for reductions in industrial emissions (Cowling et al. 2007), in NO_X emissions by power plants (e.g., Frost et al. 2006; Cowling et al. 2007), and in motor vehicle emissions (Parrish 2008).

A critical question is whether any improvement in air quality is discernable between the two campaigns, as a result of emission reductions. Studies currently in progress, however, are indicating significant

Corresponding author address: Robert M. Banta, NOAA/ESRL –CSD3, 325 Broadway, Boulder CO 80305, USA. Email: robert/banta@noaa.gov

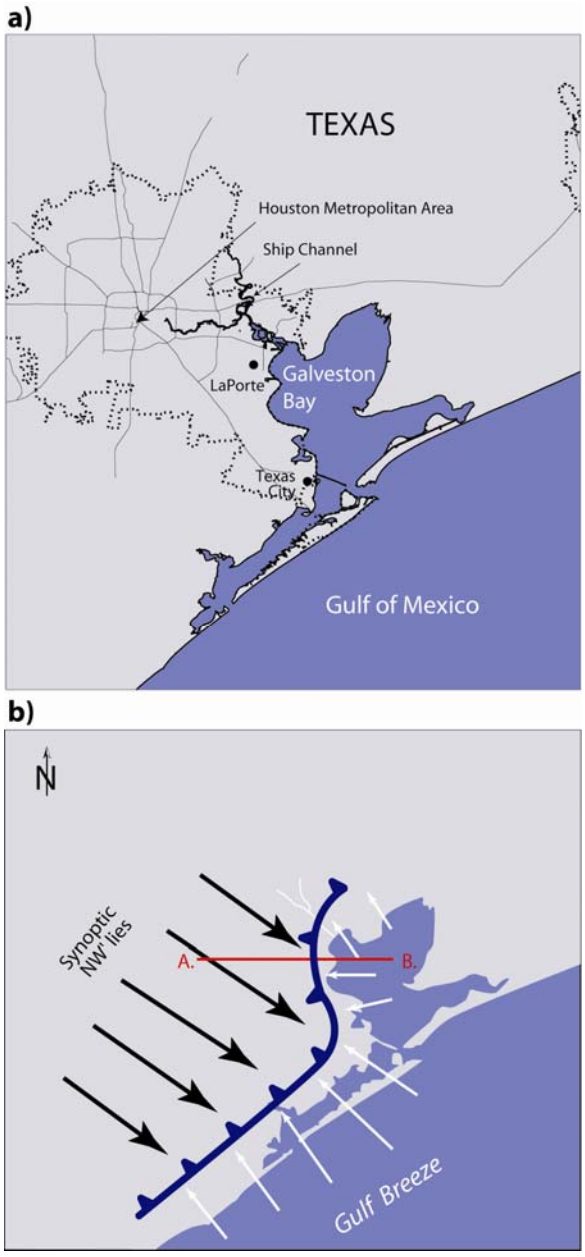

Figure 1: Maps of Houston-Galveston Bay region, a) showing urban-industrial area enclosed in the dotted line, and b) depicting the incipient sea breeze stalled along the shore of Galveston Bay, as occurred in late afternoon on 30 August 2000.

differences in meteorological conditions between the two study years (Cowling et al. 2007; Nielsen-Gammon et al. 2005). Thus, it is a goal to determine first, whether reductions in pollution levels are discernable and second, if any reductions noted may be identifiable despite the differences in meteorology between the 2000 and 2006 pollution seasons.

During the 2000 campaign the day having the highest O_3 concentrations—30 August—has been analyzed in detail (Banta et al. 2005). The high O_3 concentrations resulted from an afternoon wind shift from larger-scale offshore flow in the morning to an onshore sea breeze in late afternoon. The role of sea-breeze reversals has been well documented on many individual high-pollution days(SAI 1995, Darby 2005; Zhang et al. 2007). The necessity for such a reversal in the generation of high O_3 has been controversial, however, because relatively high O_3 has been observed on some stronger-wind days with no sea-breeze reversal, notably 6 September 2000. Thus, another issue is whether days such as 30 August and 6 September 2000 were anomalies or reflect a systematic trend.

Over relatively simple topography, atmospheric concentrations of pollutants (such as O_3) have been found to be inversely related to the BL wind speed U and the BL depth *h* (Weil, 1979; Pasquill and Smith 1983). But in the Houston-Galveston-Bay area, the coastline topography is not simple (Fig. 1), and the BL winds can be variable in space and time, especially under light wind conditions (e.g., Banta et al. 2005, Darby 2006); *h* is also highly variable. The basic inverse relationship, therefore, is probably modified in the complex wind field and BL structure of the Houston area, but some dependence on at least the wind speed is still expected. This is reflected in the operational forecasting expression developed by Lambeth (2006) for predicting maximum daily 1-hr O_3 concentrations in several Texas cities, including Houston:

$$[O_3]_{\max} = [O_3]_B + E \bullet \frac{(T_{\max} - T_{base}) \bullet R_S}{0.5 \bullet WS + 0.1 \bullet WS_{SR} + 1} \quad (1)$$

where $[O_3]_{max}$ is the maximum daily 1-hr O_3 concentration (ppb) and WS in the denominator of the right-hand side is the mean daytime BL wind speed (knots). Other symbols include $[O_3]_B$ the upwind background concentration, E a precursor emission factor, T_{max} the daytime maximum temperature, T_{base} the minimum temperature for significant O_3 production, R_S a total solar radiation factor for the day, and WS_{SR} the wind speed near sunrise. This expression

highlights variables that have been found useful for routine forecasting applications.

Operationally, $[O_3]_{max}$ is generally determined as the peak value found in the surface measurement network. Surface concentrations of O_3 can be viewed as a result of two sets of processes: (1) emission of precursors to the atmosphere, chemical reaction to form O_3, and downwind transport (which do not involve turbulent mixing or other surface interactions), and (2) downward mixing to the surface and interactions with the surface (e.g., dry deposition) or with fresh near-surface emissions. Processes in the second group in particular are complex, and spatially and temporally variable, adding significantly to the uncertainty (scatter) of measured daily maximum surface concentrations.

We note that this attempt to isolate critical meteorological variables can be complicated by suppressed-mixing events, in which locally suppressed turbulent mixing can lead to concentrations that seem anomalously high in the vicinity of source activity, and by high background pollutant levels, which can lead to high total pollutant concentrations even under meteorological conditions that would normally favor lower concentrations. These issues will be further discussed.

The present study addresses the effect of mean BL wind speed and depth *h* on peak daily ozone concentrations measured both at the surface and by airborne platforms available during TexAQS2000 and –2006. The airborne measurements have the advantage that they are not constrained to fixed locations as are surface-network measurements, but have the mobility to find the location of the highest O_3 concentrations. Moreover, they sample the O_3 concentrations aloft, avoiding the complex interactions of the second group of processes relating to surface interactions.

Data sources and analysis. Ozone data were obtained from airborne platforms and surface mesonet sites. Two kinds of airborne data are available for both campaigns, a downward-looking, ozone-profiling differential-absorption lidar (DIAL) system flown on a DC-3 (2000) and a Twin Otter (2006), and a comprehensive array of in-situ sensors assembled by NOAA/ESRL and collaborators and flown on an Electra (2000) and a P-3 (2006), which are essentially the same airplane.

The differential absorption technique consists of transmitting pulses of light (ultraviolet in this case) at two or more wavelengths selected to be at different positions on an absorption band for the species to be measured—here ozone. O_3 concentration as a function of range is calculated from the ratios of the returned signals (e.g. Browell et al., 1985). The O_3 DIAL flown in 2000 is described by Alvarez et al. (1997), Banta et al. (1997), and Senff et al. (1997), and the lidar flown in 2006 was a new, upgraded system with similar capabilities (Alvarez et al. 2008). Besides upgraded, more robust, smaller and lighter hardware, the new system provides for wavelength tunabilty of the signal to allow selection of the most suitable DIAL wavelength pair for a given atmospheric ozone and aerosol loading and to minimize interference from other species, such as sulphur dioxide.

The range-resolved, nadir-pointing beam provides a curtain of O_3 concentrations as the aircraft flies along its flight track (Fig. 2a). The lidar signals were averaged over 10-s intervals along the flight track, which translates to ozone profiles every 600 m at the ~60 m s^{-1} flight speed of the airplane. Vertically the signals were averaged over 90 m and a five-gate gliding window was then used to compute ozone. Thus, although O_3 profiles are reported at 90-m vertical resolution, truly independent data points are spaced 450 m apart. Near the ground, data from the lowest range gate straddling the surface were eliminated from further analysis. At the first point above the surface, smoothing was performed over a two-point (uncentered) window, and at the second point above the surface a three-point centered smoothing window was used. As part of our evaluations, we looked at the information from these lower two points just above the surface, but they were not used in Figs. 2-3 or in the analyses presented in this paper.

Intercomparisons with airborne in-situ data for the 2000 system indicated a root-mean-square precision of 11 ppb near the surface, improving to 3 ppb nearer to the flight level of the airplane (Alvarez et al. 1997). Preliminary comparisons with the new 2006 system indicate similar precision. The lidar signal does not penetrate clouds, so in regions of broken cloudiness we flew in clear slots between clouds as much as possible, regions of solid undercast cloudiness were avoided, and we did not fly on days when widespread rain was forecast.

The airborne DIAL data were processed by 1) identifying the flight-leg cross section with the highest O_3 concentration, and focusing in on the

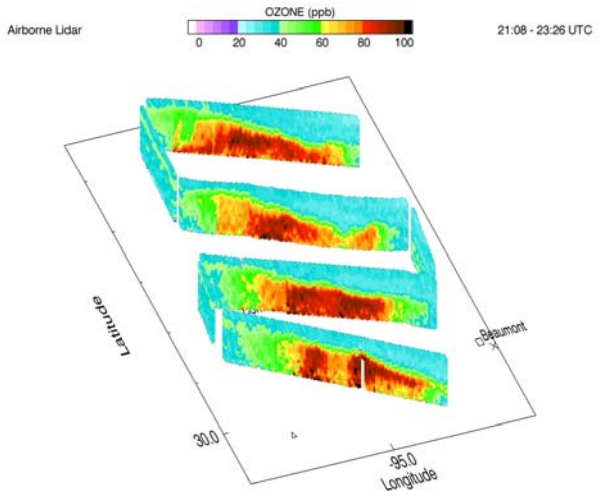

Figure 2: a) Example of the data available from the airborne ozone DIAL, using the flight of 14 August 2006, and showing the vertical and horizontal O_3 distribution for the four crosswind flight legs on that day. O_3 concentrations (ppb) are depicted in color, with color bar at top of the panel (0-100 ppb). The maximum O_3 concentrations were found on the second flight leg from the bottom, which is reproduced in Fig. 3a. Height of the measurements extends from 300 to 2000 m.

plume area of that cross section (refer to Fig. 2), then 2) calculating a mean profile for the segment of 1-4 min containing the very highest O_3 values in the plume (Fig. 3a-c). Finally, 3) the peak O_3 value of this profile (representing the highest O_3 concentration for the flight) was identified as $[O_3]_{max}$ for the DIAL data that day (Fig. 3d-f). The averaging process smoothed out data that were occasionally noisy and produced a statistically more significant value, which was representative of a broader region than the individual DIAL profiles. Some profiles appeared reasonably well mixed in the vertical, such as Fig. 3c,d, but others were not, for example Fig. 3e.

The boundary layer depth *h* was determined using range-square corrected signal (*rcs*) data from the aerosol channel (an extra, longer-wavelength channel with much-reduced O_3-absorption properties, for which attenuation is mostly due to aerosol scattering). The *rcs* for the aerosol backscatter was obtained at 6-m vertical and 10-s horizontal resolution. The magnitude of the *rcs* depends largely on the aerosol backscatter coefficient, and thus *rcs* profiles reflect the vertical distribution of aerosols. We retrieved *h* by employing a Haar-wavelet-based method (Davis et al.1999) to identify the strongest positive gradient in each 10-s *rcs* profile. The altitude at which this gradient occurred was used as an estimate of *h*. This method requires a sufficient contrast in aerosol loading between the free troposphere and the BL, and assumes higher aerosol loading in the BL than above it (Tucker et al. 2009). The BL depth presented here was evaluated over the same flight-interval location where $[O_3]_{max}$ was found, as indicated by the regions between the vertical bars in Figs. 3a-c.

In-situ measurements on the airborne platforms have been described by Ryerson et al. (2003) for the 2000 measurements and by Neuman et al. (2006) for the 2006 measurements. O_3 was measured by a chemiluminescence detector at a sampling rate averaged to 1 Hz. Uncertainties in these measurements were determined to be +/- (0.3 ppb + 3%) for the instrument flown in 2000, and +/- (0.1 + 3%) for the 2006 instrument.

Surface O_3 values averaged over 1-hr were available in 2000. Five-minute values were available in 2006, so for purposes of comparing the best available ground data with the airborne data, these data were used in 2006, even though this difference in sampling procedure precludes a rigorous comparison of O_3 maxima for the two years using surface measurements. We did, however, find evidence for improvements in the sampling abilities of the expanded, higher-time-resolution network in 2006 as compared with the 2000 dataset.

Peak O_3 on a given day is a result of Houston-area emissions being added to background O_3 concentrations $[O_3]_B$, which may be advected in from distant regions or may accumulate locally during stagnation episodes. The daily increment or "add on" contribution $[O_3]_A$ by the Houston urban-industrial region is the peak O_3 minus the background value, or $[O_3]_A = [O_3]_{max} - [O_3]_B$. Although background concentrations are observed to vary horizontally and to increase in time through a daylight period, for uniformity of analysis among the study days we use an objective method described by Nielsen-Gammon et al. (2005) for calculation of $[O_3]_B$. A ring of five surface-measurement sites surrounding the Houston area was selected so that each site was well outside the direct influence of source activity—i.e., at a distance where titration of O_3 by fresh

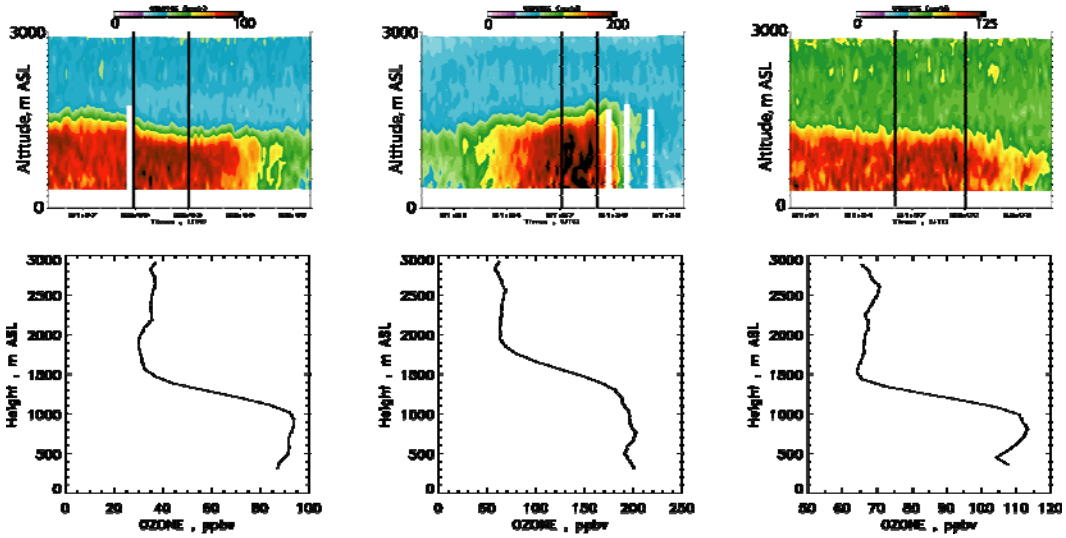

Figure 3. Method for determining peak daily O_3 is illustrated in this figure. The flight leg containing the highest O_3 values was selected for each day, e.g., a) represents the leg with the peak $[O_3]$ for 14 August 2006, b) is the leg for 16 August 2006, and c) is the leg for 30 August 2006. The 2-4-min segment of each flight leg containing the highest O_3 was identified, as indicated by the vertical black bars on each leg, and the data were averaged horizontally across the segment to form profiles, as shown in panels d)-f). The maximum value for each profile was then selected as the estimate for $[O_3]_{max}$, the maximum O_3 concentration for that day.

urban or industrial emissions should not be a factor. The locations of these sites have been plotted on a map of the Houston area by Rappenglück et al. (2007). For each day, the smallest of the five 8-hr maximum O_3 concentrations for this ring was taken as the background value. Advantages of this approach were that it is an objective method and it provides a uniform background dataset for all days. The lowest background values observed during 2006 were 16-21 ppb on five days of the 24-day airborne sample (12, 14, 15 August and 15, 21 September).

Winds in the BL were measured by an array of 915-MHz radar wind profilers, which provided hourly-averaged winds with a vertical resolution of 60 m at a precision of 1 m s^{-1} (Martner et al.1993), starting at a height of ~150 m. An important consideration is over what time interval to average these winds, which were also vertically averaged between 200 and 500 m. On the highest pollution days, such as 30 August 2000 (Banta et al. 2005), morning offshore flow is often relatively stiff (several m s^{-1}) until the sea-breeze reversal, and then an hour or so after the sea-breeze frontal passage (reversal), the sea breeze itself can be several m s^{-1}, even near the surface. A straightforward scalar average of the wind speed is likely to unduly emphasize the stronger winds before and after the reversal period on many days. Moreover, the timing of the sea-breeze frontal reversal varied from day to day, making it difficult to define a consistent averaging time of day that would bracket this period.

It has been argued that an important aspect of the pollution-accumulation process in the BL is recycling of morning emissions and the occurrence of light winds of variable direction during the sea-breeze frontal stagnation period (STI et al. 1995; Banta et al. 2005; Darby 2005; Zhang et al. 2007). To account for all the various dynamic processes affecting the peak pollutant concentrations, we use a vector-averaged wind speed <U>. The vector average is calculated as the net displacement of the trajectory based on the 200-500-m mean wind, starting at Houston (29.7687° N, 95.3867° W) at 1400 UTC [0900 Central Daylight Time (CDT), at the end of the morning rush hour] and extending over a period of 10 hr, then dividing the displacement by the time interval. Steady winds produce a straight trajectory, for which the vector- and scalar-average speeds are equal, whereas variable winds with significant directional changes in time produce crooked trajectories with the vector-averaged wind smaller than the scalar average. This reduction for the vector average represents recycling effects and the movement of air back and forth over the various emission sources.

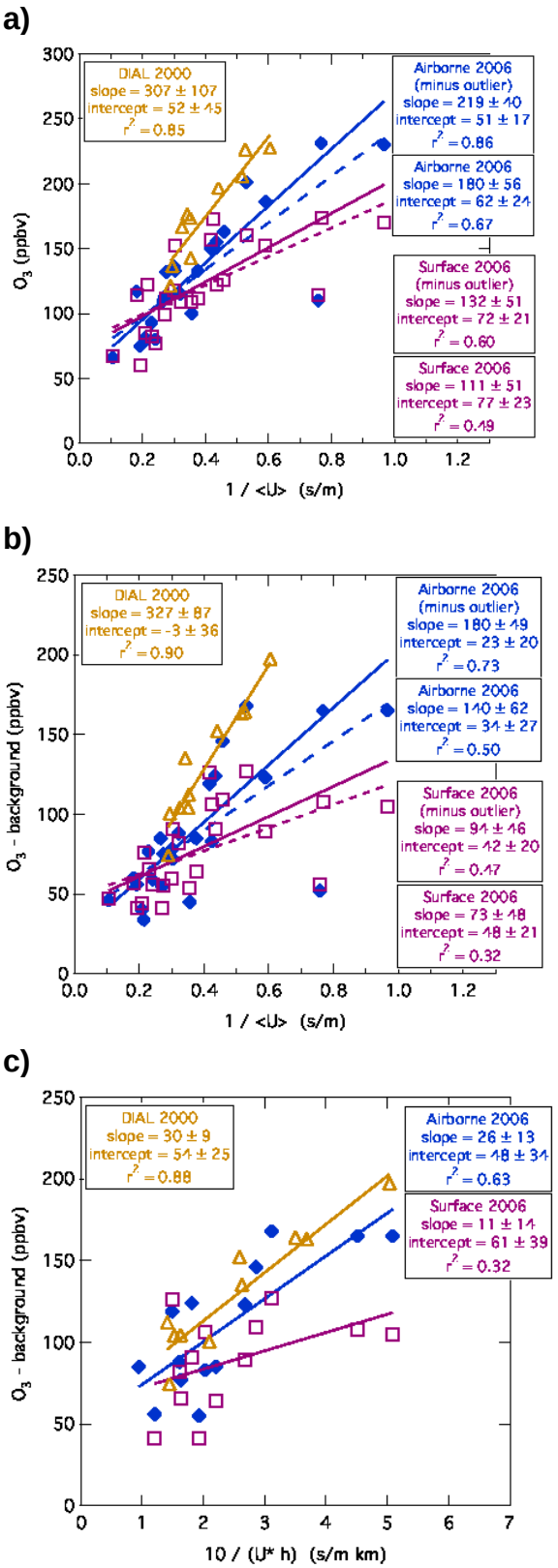

Figure 4. a) Maximum daily ozone $[O_3]_{max}$ plotted vs. inverse of vector-averaged wind speed $<U>^{-1}$ for the study days in 2000 and 2006, and least-squares regression line is indicated (solid). b) Same as a), except daily maximum Houston-area add-on contribution $[O_3]_A$ plotted vs. $<U>^{-1}$. c) $[O_3]_A$ vs. $<Uh>^{-1}$ includes the BL depth h in the abscissa. d) $[O_3]_A$ vs. $T_{max} / <U>^{-1}$ includes the daily maximum temperature at an urban site in the abscissa. In each panel, the gold data and line are from the 2000 airborne DIAL measurements, the dark blue are for the 2006 airborne (DIAL and P-3) measurements, and the red are for the 2006 surface-array measurements. The 2000 airborne Electra and surface measurements showed considerable scatter, as indicated by the r^2 correlations (Table I), and were not plotted here to improve the clarity of the plots.

The 10-hr averaging interval includes any wind reversal important to daytime air quality and adequately samples the flow before and after the reversals. We also tried using 5-hr trajectories starting an hour later, but on high pollution days such as 30 August 2000, effects of the late-day sea breeze flow were not well represented.

Results. We investigate the relationship between peak daily ozone and wind speed by plotting $[O_3]_{max}$ and the Houston-area ozone add-on contribution $[O_3]_A$ as functions of the vector-averaged wind speed. The expected reciprocal relationship between $[O_3]_{max}$ and $<U>$ (e.g., Eq. 1) is illustrated by plotting peak ozone vs. $<U>^{-1}$ (Fig. 4a). The 2000 airborne DIAL

data (gold line) show a strong correlation with $<U>^{-1}$ (r^2 = 0.85: see Table 1). The 2006 airborne data (blue line), which include both DIAL and P-3 (in-situ) data, likewise indicate a strong correlation (r^2=0.86). Surface $[O_3]_{max}$ data show correlation but with greater scatter (r^2=0.60 for 2006, and, =0.27 for 2000; see Table I), reflecting the complex process and sampling issues discussed previously.

Peak daily O_3 values for each type of data were also plotted against the wind speed <U> itself, as listed in Table I (not plotted). The 2000 DIAL and 2006 airborne (DIAL plus P-3) data indicate a strong negative linear correlation with the independent variable, this time <U> (r^2 of 0.89 and 0.77, respectively). As before, the peak ozone at the surface is correlated (negatively) but with greater scatter (r^2=0.61 for 2006) than the airborne data.

The strong correlations of the *peak* daily O_3 with wind speed were somewhat unexpected, given that background O_3 values ranged from 16 to 67 ppb. Fig. 4b shows the Houston-area add on $[O_3]_A$ plotted against the inverse wind speed. The 2000 DIAL data continue to show strong correlation (r^2=0.90). Correlation is also evident in the 2006 airborne data, but less strongly for the add-on data (r^2=0.73) than was evident for the daily maximum O_3 data. The correlation for the surface $[O_3]_A$ dataset again shows more scatter than the airborne data, and this correlation is also weaker than for the $[O_3]_{max}$ data for 2006. Correlation statistics for other combinations of data were calculated, and the correlation results for these trials are shown in Table I.

Figure 4c shows the effect of including the BL depth *h* in the denominator of the abscissa, which becomes $<Uh>^{-1}$. The effect is to degrade the correlation, as r^2 decreases to 0.63 (from 0.73) for the 2006 airborne data sets. Table I shows that this degradation was generally true for the other correlations calculated. The implication is that in general peak O_3 concentrations were most strongly controlled by factors other than *h*. This is consistent with other findings (e.g., Cowling et al. 2007; Rappenglück et al. 2008). Thus, factors controlling *h* were generally different from factors controlling maximum ozone concentrations, especially in the complex coastal environment where *h* exhibits strong spatial variability.

We also attempted to correlate peak O_3 against the maximum afternoon temperature T_{max} . Temperature affects O_3 concentrations in a complex manner, including the rates of the chemical and photochemical reactions, and rates of biogenic and anthropogenic emissions (e.g., Sillman and Samson 1995), so that the temperature dependence of ozone is likely to be regionally and seasonally variable. For our dataset, T_{max} and $[O_3]_{max}$ were found to be essentially uncorrelated for 2000 (r^2 values <0.02) and weakly correlated for 2006 (r^2 = 0.3 and 0.5 for $[O_3]_{max}$ and $[O_3]_A$). This is further reflected in the correlations between O_3 and T/<U>, which have values similar to the correlations with 1/<U> (Fig. 4d and Table 1). In other words, considering the effects of temperature had little effect on the correlations.

Discussion. The relationships in the plots in Fig. 4 show most obviously that peak ozone concentrations were highest for the lowest wind speeds, i.e., the "theoretical" overall inverse relationship between peak daily ozone and wind speed held true, even in the complex coastal environment of the Houston area, when the winds were appropriately averaged. Two effects produce the higher concentrations at the lower wind speeds: first, the effect of wind speed vs. emission rate on dilution at the source, which also occurs in steady flow over simple topography, and second, the occurrence in the coastal environment of sea-breeze and associated wind-reversal /pollutant recirculation activities at lower ambient wind speeds. Sea-breeze development is suppressed by strong large-scale winds.

For the overall sample, the very highest O_3 concentrations occurred at the lowest wind speeds. Specifically, Houston-area add-on O_3 contributions greater than 150 ppb only occurred for <U> less than 2 m s^{-1} (or $<U>^{-1}$ greater than 0.5 s m^{-1}). High background concentrations can lead to high total daily $[O_3]_{max}$, but for this dataset, days with $[O_3]_{max}$ greater than 200 ppb measured in the BL also only occurred when <U> was less than 2 m s^{-1}. This light-wind criterion, reflecting sea-breeze wind-shift occurrences, does not seem to be a *sufficient* condition for the very high concentrations, however, since some days with such low wind speeds did not produce the extreme concentrations (e.g., 26 September 2006 and 31 August 2006). Large-scale wind direction and cloudiness, not considered in this analysis, are other important factors being investigated in studies of individual cases.

This relationship between weak winds and high ozone was true for each type of data

examined, including airborne lidar, airborne in-situ, and surface in-situ measurements. The expected reciprocal $\langle U \rangle^{-1}$ relationship was especially strong for the 2000 airborne DIAL data. The apparent negative-linear relationship (i.e., vs. <U>), which may represent the ascending branch of a hyperbolic function (characteristic of $\langle U \rangle^{-1}$), was also strong. Of possible interest for forecasting schemes is the fact that airborne data from 2006 were actually better represented by the negative-linear relationship between ozone concentrations and <U> than the reciprocal relationship $\langle U \rangle^{-1}$ for both peak O_3 and add-on. This also reinforces the fact that the relationship between ozone and wind speed is not a simple one, but a result of diverse interactions among chemical and dynamic processes in the complex coastal setting. But the high r^2 correlation values, representing the fraction of the variance of peak or add-on O_3 concentrations accounted for by their association with wind speed, show that the meteorological factor most strongly related to peak daily O_3 values in the Houston area was the vector-averaged wind speed <U> (or its reciprocal).

An inverse relationship between *h* and $[O_3]_{max}$ seems almost intuitive, so their lack of correlation warrants further discussion. Obviously, in any given O_3 profile, if *h* had been 20% higher, for example, $[O_3]$ would have been correspondingly lower, since O_3 typically tends to be mixed through the daytime BL. But more generally, O_3 concentrations are controlled by one set of meteorological factors, and *h* is controlled by another set of factors. The primary controls on O_3 concentrations were U and sea-breeze development, according to the results given here, whereas the primary controls on *h* include factors related to the surface heat flux via the surface energy budget, the pre-existing stratification (e.g., previous day's *h*), and others (Tennekes 1973, Banta and White 2003). To be sure, one of the factors controlling O_3 concentration is *h*, but the weak correlations show that this is a secondary effect most of the time. Scatter diagrams (Fig. 5) between *h* and O_3 for the 24-day dataset of this study indicate low correlations (r^2 values of 0.06 or less). These plots show that *h* was often 1.5 km +/- 250 m. Over this band of *h* values, $[O_3]_{max}$ varied in a random-appearing fashion between 60 and 200 ppb, and $[O_3]_A$ varied from 40 to 150 ppb also unsystematically, illustrating the

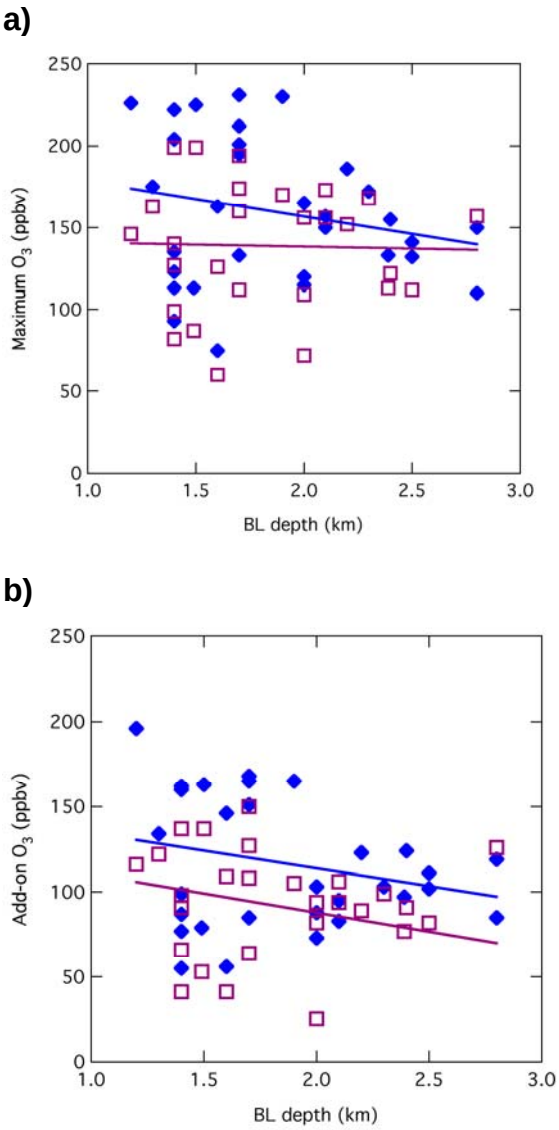

Figure 5. a) Peak daily ozone $[O_3]_{max}$ for both years plotted vs. boundary-layer depth h, with least-squares regression line indicated. b) Same as a), except ordinate is Houston-area add-on contribution $[O_3]_A$.

difficulty in using *h* as a predictor for daily peak ozone.

This is not to say that *h* never exerts a stronger influence on $[O_3]$. Under specific circumstances (especially flow over Galveston Bay or the Gulf of Mexico) suppressed *h* or otherwise suppressed vertical mixing can lead to higher $[O_3]$. For example, during morning offshore flow from the Houston urban/Ship-Channel source region to Galveston Bay and the Gulf of Mexico, airborne DIAL cross sections show high concentrations of Houston-area

pollutants confined to a layer less than 600 m deep over Galveston Bay (Banta et al. 2005; see Fig. 6b of that paper), corresponding to the typical BL depth there (Tucker et al. 2009). Another exception was a case of high $[O_3]$ found by the Electra aircraft on 1 September 2000 near the eastern, downwind shore of Galveston Bay. An O_3 concentration of 245 ppb, found within an elevated plume above the Galveston-Bay marine BL, was confined by the stratification to a layer of a depth of 500 m, as measured by the airborne DIAL. Altogether for the Electra's $[O_3]$ vs. $\langle U \rangle$ or $\langle U \rangle^{-1}$ datasets in 2000, correlations (r^2) were low (Table 1), largely because of the anomalously high O_3 concentrations for the wind speed on 1 September and some other days. When corrected for the limited depth of mixing (by setting h = 500m in $\langle Uh \rangle^{-1}$), the data for these days fell in line with the other points, and the correlations improved to ~0.7 or greater (Table 1). In fact, corresponding slope and bias values show that the airborne DIAL and Electra regressions became nearly collinear. In these specific instances, therefore, vertical depth of mixing did exert a significant control on maximum ozone concentrations. But in the broader sense illustrated by Fig. 4, h did not display a strong primary influence on $[O_3]_A$ or $[O_3]_{max}$.

Other findings from Fig. 4 and Table I include the following.

- The relatively high total ozone concentrations found on stronger-wind days (e.g., 165 ppb on 6 September 2000) were not significant outliers, particularly when high background values are accounted for.
- Surface ozone concentrations were routinely less than airborne values, at least in part because of sampling limitations of the surface network. For example, on 12 August 2006, the urban plume was observed by the airborne DIAL just to the east of Conroe, Texas, but was completely missed by the network. Another factor is the complex surface-interaction (including removal) processes, which most likely contribute to the scatter in the surface measurements of daily maximum values, as previously described.
- The scatter is larger (r^2 smaller) for the surface values than for the airborne, but the scatter for surface sampling was less so (r^2 larger) in 2006 than in 2000, suggesting that the broader measurement network and the use of 5-min data improved the sampling.
- Day in and day out, h was not found to be a strong predictor of peak daily ozone. More skill may be demonstrated if other predictors were included, such as mean BL wind direction, but a larger dataset would be required to further stratify the available data.

One of the ultimate goals for the understanding gained from air-quality research studies such as this one is to be able to predict peak ozone concentrations several hours to days in advance. The predictor in this study, the vector-averaged wind speed aloft, is not a routine or easily predictable variable, as it involves the location, timing, and intensity of the along-shore sea-breeze reversal zone (front). The best hope for predictions of such a quantity would be from high-resolution mesoscale numerical weather prediction (NWP) model output. A critical question is, can current-generation models routinely provide quantitative predictions of these processes on a daily basis, without adjustment of model constants or other parameters, with sufficient fidelity? It has been argued that improvement in the representation of a number of physical processes will be needed before models can be relied upon to provide this level of predictive accuracy (Dabberdt et al. 2004, Seaman 2000, Bao et al. 2005, Banta et al. 2005).

Another area where research is needed is in the relationship between concentrations of pollutants aloft and those at the surface, where human activity takes place. In this study we have been able to establish a strong relationship between wind speed and maximum daily ozone concentrations aloft using aircraft data, but how, where, and whether this ozone impacts the surface involves physical transport and mixing processes that are not well understood, and not well represented in models, especially in complex environs such as the Galveston Bay/Gulf of Mexico coastline. The increased scatter in the surface measurement-network data over the airborne data is an indication that these processes are important, but they need to be better understood.

Conclusions. The analyses in this paper for 2000 and 2006 have shown that meteorological factors controlling the peak daily O_3 concentration were well represented by the vector-averaged wind speed, accounting for 80-90% of the O_3 variance. At the lowest wind speeds, for a given value of $\langle U \rangle$, peak O_3 values in 2000 were higher than in 2006. This

difference decreased to 'no discernable difference' as speeds increased to greater than 5 m s^{-1}. In other words, the worst pollution days were worse in 2000 than 2006 for a given value of <U>, the effect being most evident on the lowest wind-speed, highest-pollution days. Because the meteorological factor most strongly associated with high O_3 was <U> for both years, the analysis (Fig. 4), in which the best-fit line for 2000 is everywhere above the line for 2006 until they converge at 5 m s^{-1}, takes the differences in meteorology between the two years into account. Similar plots using only DIAL, and ones using only surface data, for both years show similar improvements for 2006.

These findings thus indicate that pollution emissions were less in 2006 than in 2000, suggesting that control measures implemented between the two campaigns have been effective. That the improvement is greatest on the weakest-wind days is a favorable outcome, since these are the days that present the most severe health risks over the most densely populated areas. It is important to note, however, that even though improvement was less discernible on the stronger wind days, it still must be the case that less net ozone was being produced in 2006 even on these days, as a result of lowered emissions. Since the Houston area is a prodigious source of pollution to the surrounding regions, the consequences of the reduced emissions even on the stronger-wind days would include reductions of background ozone for other regions of Texas and the surrounding regions of the United States. Houston is still an area that is in nonattainment for the national air quality standards, because the concentration levels of major pollutants including ozone are still high. Continued improvement is therefore required.

REFERENCES

Alvarez R.J., II, C.J. Senff, R.M. Hardesty, D.D. Parish, W.T. Luke, T.B. Watson, P.H. Daum, and N. Gillani, 1997: Comparisons of airborne lidar measurements of ozone with airborne in situ measurements during the 1995 Southern Oxidants Study, *J. Geophys. Res*. **103**, 31,155-31,171.

Alvarez II, R. J., W. A. Brewer, D. C. Law, J. L. Machol, R. D. Marchbanks, S. P. Sandberg, C. J. Senff, A. M. Weickmann, 2008: Development and application of the TOPAZ airborne lidar system by the NOAA Earth System Research Laboratory, Proceedings of *24th International Laser Radar Conference*, Boulder, Colorado, USA, 23-27 June, 2008, 68-71.

Banta, R.M., C.J. Senff, A.B. White, M. Trainer, R.T. McNider, R.J. Valente, S.D. Mayor, R.J. Alvarez, R.M. Hardesty, D.D. Parish, and F.C. Fehsenfeld, 1998: Daytime buildup and nighttime transport of urban ozone in the boundary layer during a stagnation episode. *J. Geophys. Res.*, **103**, 22,519-22,544.

Banta, R.M., and A.B.White, 2003: Mixing-height differences between land-use types: Dependence on wind speed. *J. Geophys. Res.*, **108** (D10), 4321, doi: 10. 1029/2002JD002748.

Banta, R.M., C.J. Senff, T.B. Ryerson, J. Nielsen-Gammon, L.S. Darby, R.J. Alvarez, S.P. Sandberg, E.J. Williams, and M. Trainer, 2005: A bad air day in Houston. *Bull. Amer. Meteor. Soc.*, **86**, 657-669.

Bao, J.-W, S.A. Michelson, S.A. McKeen, and G.A. Grell, 2005: Meteorological evaluation of a weather-chemistry forecasting model using observations from the TEXAS AQS 2000 field experiment. *J. Geophys. Res.*, **110**, D21105, doi:10. 1029/2004JD005024.

Browell, E.V., S. Ismail, and S.T. Shipley, 1985: Ultraviolet DIAL measurements of O_3 profiles in regions of spatially inhomogeneous aerosols. *Applied Optics,* **24**, 2827-2836.

Cowling, E.B., et al. 2007: Final Rapid Systhesis Report: Findings from the Second Texas Air Quality Study (TexAQS II). Final Report, TCEQ Contract No. 582-4-65614, Texas Commission on Environmental Quality, Austin, Texas, pp. 143.

Dabberdt and Coauthors, 2004: Meteorological research needs for improved air quality forecasting. *Bull. Amer. Meteor. Soc.*, **85**, 563-586.

Darby, L.S., 2005: Cluster analysis of surface winds in Houston, Texas and the

impact of wind patterns on ozone. *J. Appl. Meteor.*, **44**, 1788-1806.

Davis, K. J., N. Gamage, C. R. Hagelberg, C. Kiemle, D. H. Lenschow, and P. P. Sullivan, 1999: An Objective Method for Deriving Atmospheric Structure from airborne lidar observations. *J. Atmos. Ocean. Technol.*, **17**, 1455-1468.

Frost, G. J., S. A. McKeen, M. Trainer, T. B. Ryerson, J. A. Neuman, J. M. Roberts, A. Swanson, J. S. Holloway, D. T. Sueper, T. Fortin, D. D. Parrish, F. C. Fehsenfeld, F. Flocke, S. E. Peckham, G. A. Grell, D. Kowal, J. Cartwright, N. Auerbach, and T. Habermann, 2006: Effects of changing power plant NO_x emissions on ozone in the eastern United States: Proof of concept. *J. Geophys. Res.*, **111**, D12306, doi:10.1029/2005JD006354.

Lambeth, B., 2006: Ozone maximum model forecast version. National Air Quality Conf., February 2006.

Martner, B., D.B. Wuertz, B.B. Stankov, R.G. Strauch, E.R. Westwater, K.S. Gage, W.L. Ecklund, C.L. Martin, and W.F. Dabberdt, 1993: An evaluation of wind profiler, RASS, and microwave radiometer performance. *Bull. Amer. Meteor. Soc.*, **74**, 599-613.

Neuman, J.A., et al., 2006: Reactive nitrogen transport and photochemistry in urban plumes over the North Atlantic Ocean. *J. Geophys. Res*. **111**, D23S54, doi:10.1029/2005JD007010.

Nielsen-Gammon, J., J. Tobin, A. McNeel, and G. Li, 2005: A conceptual model for eight-hour exceedances in Houston, Texas. Part I: Background ozone levels in Eastern Texas. Report, Center for Atmospheric Chemistry and the Environment, Texas A&M University, College Station TX, 52 pp.

Parrish, D.D., 2008: Critical evaluation of U.S. on-road vehicle emission inventories. *Atmos. Environ.*, **40**, 2288-2300.

Pasquill, F., and F. B. Smith, 1983: *Atmospheric Diffusion*, 3rd Ed., Wiley, New York, 437 pp.

Rappenglück B., R. Perna, S. Zhong, G.A. Morris, 2008: An analysis of the vertical structure of the atmosphere and the upper-level meteorology and their impact on surface ozone levels in Houston, Texas. *J. Geophys. Res.*, submitted.

Ryerson et al. 2003: Effect of petrochemical industrial emissions of reactive alkenes and NO_X on tropospheric ozone formation in Houston, Texas. *J. Geophys. Res*. **108**, 4249, doi:10.1029/2002JD00307.

SAI (Systems Applications International), Sonoma Technology, Inc., Earth Tech., Alpine Geophysics and A.J. Kearney, 1995: Gulf of Mexico air quality study, final report, Vol I: Summary of data analysis and modeling. OCS Study MM5-95-0038, U.S. Dept. of the Interior, Minerals Management Service, Gulf of Mexico OCS Region, New Orleans LA, 654 pp.

Seaman, N., 2000: Meteorological modeling for air-quality assessments. *Atmos. Environ.*, **34**, 2231-2259.

Senff, C.J., R.M. Hardesty, R.J. Alvarez, and S.D. Mayor, 1997: Airborne lidar characterization of power plant plumes during the 1995 Southern Oxidants Study. *J. Geophys. Res*. **103**, 31,173-31,189.

Sillman, S. and P.J. Samson, 1995: Impact of temperature on oxidant photochemistry in urban, polluted rural, and remote environments. *J. Geophys. Res*. **100**, 11,497-11,508.

Tennekes, H., 1973: A model for the dynamics of the inversion above a convective boundary layer. *J. Atmos. Sci.*, **30**, 558-567.

Tucker, S.C., W.A. Brewer, R.M. Banta, C.J. Senff, S.P. Sandberg, D.C. Law, A.M. Weickmann, and R. M. Hardesty, 2009: Doppler lidar estimation of mixing height using turbulence, shear, and aerosol profiles. *J. Atmos. Oceanic Technol.*, **25**, in press.

Weil, J.C., 1979: Applicability of stability classification schemes and associated parameters to dispersion of tall stack plumes in Maryland. Atmos. Environ., 819--831.

Williams, E.J., B. Lerner, P. Murphy, S. Herndon, and M. Zahnser, 2009: Emissions of NOx, SO_2, CO, H_2CO and C_2H_4 from commercial marine shipping during TexAQS 2006 *J. Geophys. Res*., submitted.

Zhang, F., N. Bei, J.W. Nielsen-Gammon, G. Li, R. Zhang, A. Stuart, and A. Aksoy, 2007: Impacts of meteorological uncertainties on ozone pollution predictability estimated through meteorological and photochemical ensemble forecasts. *J. Geophys. Res.*, **112**, D04304, doi:10.1029/2006JD007429.

Table I

$[O_3]_{max}$ – Daily Maximum Ozone										
2000						**2006**				
		Slope	Bias		r^2		Slope	Bias		r^2
1 / <U>										
	DIAL	307	52		0.85	DIAL	213	55		0.90
	Electra	366	30		0.32	Airborne	219	51		0.86
	Surface	207	65		0.27	Surface	132	72		0.60
<U>										
	DIAL	-57	318		0.89	DIAL	-38	257		0.91
	Electra	-26	324		0.33	Airborne	-33	238		0.77
	Surface	-39	250		0.34	Surface	-20	188		0.61
1/<Uh>										
	DIAL	26	109		0.72	DIAL	36	64		0.80
	Electra	29	92		0.69	Airborne	36	65		0.80
	Surface	13	113		0.19	Surface	21	79		0.43
T / <U>										
	DIAL	8.3	53		0.87	DIAL	6.2	56		0.92
	Electra	10.1	28		0.38	Airborne	6.1	58		0.86
	Surface	6.0	60		0.33	Surface	3.4	79		0.54

Table 1 (continued) Urban-area add-on-contribution concentrations

$[O_3]_A$ – Houston-Area Ozone Add-on Contribution										
2000						**2006**				
		Slope	Bias		r^2		Slope	Bias		r^2
1 / <U>										
	DIAL	327	-3		0.90	DIAL	154	43		0.72
	Electra	291	15		0.24	Airborne	180	23		0.73
	Surface	198	24		0.34	Surface	94	42		0.47
<U>										
	DIAL	-56	277		0.91	DIAL	-29	192		0.79
	Electra	-47	253		0.27	Airborne	-28	180		0.70
	Surface	-36	199		0.41	Surface	-16	130		0.56
1/<Uh>										
	DIAL	30	54		0.88	DIAL	26	50		0.63
	Electra	28	51		0.76	Airborne	26	48		0.63
	Surface	14	66		0.28	Surface	11	61		0.32
T / <U>										
	DIAL	8.6	2		0.88	DIAL	4.6	42		0.76
	Electra	8.3	10		0.32	Airborne	5.2	26		0.78
	Surface	5.6	21		0.39	Surface	2.7	44		0.49